

Accurate radius and mass of the transiting exoplanet OGLE-TR-132b [★]

Moutou C.¹, Pont F.², Bouchy F.¹, Mayor M.²

¹ LAM, Traverse du Siphon, BP8, Les Trois Lucs, 13376 Marseille cedex 12, France

² Observatoire de Genève, 51 Chemin des Maillettes, 1290 Sauverny, Switzerland

Received date / accepted date

Abstract. The exoplanet OGLE-TR-132b belongs to the new class of very hot giant planets, together with OGLE-TR-56b and OGLE-TR-113b, detected by their transits. Recently, radial velocity measurements provided a planetary mass estimate for OGLE-TR-132b. The planet parameters, however, were poorly constrained, because of the very shallow transit in the OGLE light curve. In this letter, based on new VLT/FORS2 photometric follow-up of OGLE-TR-132 of unprecedented quality (1.2 millimagnitude relative photometry), we confirm the planetary nature of the orbiting object, and we derive an accurate measurement of its radius and mass: $1.13 \pm 0.08 R_J$ and $1.19 \pm 0.13 M_J$. The refined ephemeris of OGLE-TR-132 transits is $T_0 = 2453142.5888$ and $P = 1.689857$ days.

Key words. planetary systems - stars: individual: OGLE-TR-132

1. Introduction

The rich complementarity of transit and radial-velocity methods in the detection and study of extrasolar planets has opened the way to characterizing some of these planets. It is now possible in particular to investigate the mass-radius relationship of extrasolar giant planets. The first transiting exoplanet HD209458b (Charbonneau et al. 2000, Henry et al. 2000) has been extensively observed, up to the recent detection of its exosphere (Vidal-Madjar et al. 2003). Several transiting hot Jupiter candidates were detected by OGLE (Optical Gravitational Lensing Experiment, Udalski et al. 2002a, 2002b, 2003) and three of them were confirmed by radial-velocity follow-up: OGLE-TR-56b (Konacki et al. 2003), OGLE-TR-113b (Bouchy et al. 2004, Konacki et al. 2004) and OGLE-TR-132b (Bouchy et al. 2004, hereafter referenced as "BPS"). The low orbital periods of these three planets (less than 1.7 days) make them extreme cases of the "hot Jupiter" class. They have radii and masses consistent with one another and markedly higher density than HD209458b (Brown et al. 2001).

The transit dip of OGLE-TR-132 in the OGLE light curve is very shallow compared to the mean photometric error bars ($d \sim 0.008$, $\sigma \sim 0.006$), providing little constraints on the parameters of the transit, in particular the

impact parameter. BPS show that the data was consistent with a central transit of a $R \sim 1.3R_\odot$ star by a $r \sim 1R_J$ planet, but also with a high-latitude transit of a much larger star by a larger planet.

The reality of the transit and radial velocity signals themselves were not entirely beyond doubt. OGLE-TR-132 belongs to a "supplement" of very shallow signals detected in the OGLE data with the BLS algorithm (Kovács et al., 2002) which also includes at least one object with no radial velocity signal (OGLE-TR-131, BPS) that can be suspected to be a false positive. Moreover, BPS estimate that the radial velocity signal of OGLE-TR-132 has a 3% chance of being due to random fluctuation in the velocity residuals.

In this letter, we present a much more accurate light curve of the transit of OGLE-TR-132, obtained with the FORS2 imager on the VLT. The new data unambiguously confirm the reality of both the photometric transit and radial velocity signal, and allow precise constraints to be put on the shape and phasing of the transit, therefore yielding much improved radius and mass determinations for the planetary companion.

2. Observations and data reduction

The observations were obtained during 4 hours on May 16th, 2004 on the FORS2 camera of VLT/UT4 (programme 273.C-5017A). In total, 281 short exposures (15-20 sec) in the $R_{special}$ filter were acquired, in a $3.4' \times 3.4'$ field of view around OGLE-TR-132. Two images in the Bessel V filter were acquired before and after the long

Send offprint requests to: Claire.Moutou@oamp.fr

[★] Based on observations collected with the FORS2 imager at the VLT/UT4 Yepun telescope (Paranal Observatory, ESO, Chile) in the DDT programme 273.C-5017A.

$R_{special}$ sequence, for colour calibration. We used FORS2 with the high-resolution collimator and a 2×2 pixel binning in order to get both spatial sampling and short read-out time. The pixel size is $0.12''$. The atmospheric conditions during the observed sequence were excellent and stable: the average seeing at zenith is $0.55''$ with up to 20% fluctuations, and transparency was high and stable. The airmass of the field grows from 1.26 to 1.58 during the sequence. We obtained approximately one photometric measurement per minute with exposure times of 15 or 20 seconds; the sequence was scheduled following recent radial velocity measurements which suggested a possible shift of up to 4 hours from the OGLE ephemeris (BPS).

The frames were debiased and flatfielded with the standard ESO pipeline. In the following, only the chip 1 where OGLE-TR-132 lies is mentioned (half of the field of view). Differential photometry was performed with the image subtraction algorithm (Alard & Lupton, 1998 and Alard, 2000). The combination of the three best-quality images led to the creation of the reference frame. After an astrometric interpolation of all images (3rd-degree polynomial fitting of the distortions), all images are then scaled to the reference using adapted kernels to compensate for the varying seeing and background conditions. Aperture photometry is then performed with the DAOPHOT package in IRAF (Stetson 1987) to both the reference frame and subtracted images. Different apertures were tested for the extraction, and the best compromise between including all the flux of the object and minimizing the sky background was found for an aperture of 10 pixel radius. The resulting light curve of OGLE-TR-132 is shown on Figure 1 (data are available electronically). Several tens of stars of similar colour and magnitude than OGLE-TR-132 were measured for comparison and twenty of them were selected to produce an average light curve (under conditions of low intrinsic variability, clean sky area, large brightness without saturation and low blending). This comparison light curve is then subtracted to the light curve of OGLE-TR-132 to remove residual systematics. A small second-order residual was found in the sky background subtraction between the 15-second and the 20-second exposures. This residual, amounting to 0.4 mmag for the optimal aperture of 10 pixel radius, was removed in the final light curve.

OGLE-TR-132 has a close visual companion about $1''$ to the east. We also checked that this companion was not variable: the variations of the 20-times-fainter companion are of the order of 2%, due to residuals in the PSF wing of OGLE-TR-132. Were the companion responsible for the observed transit, it should be variable by $\simeq 15\%$, which is not observed.

3. Results

3.1. Light curve analysis

The dispersion in the resulting light curve for our comparison stars is very close to the photon noise limit. The

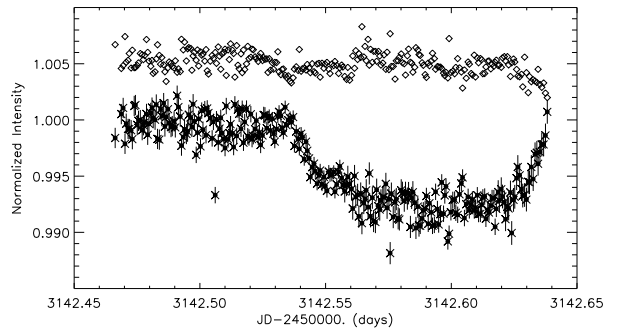


Fig. 1. Our VLT/FORS light curve for the observed transit of OGLE-TR-132. The top curve (losanges) is the mean light curve obtained from 20 stars in the field (shifted by 0.005 for clarity), from which the target light curve (bottom) is corrected.

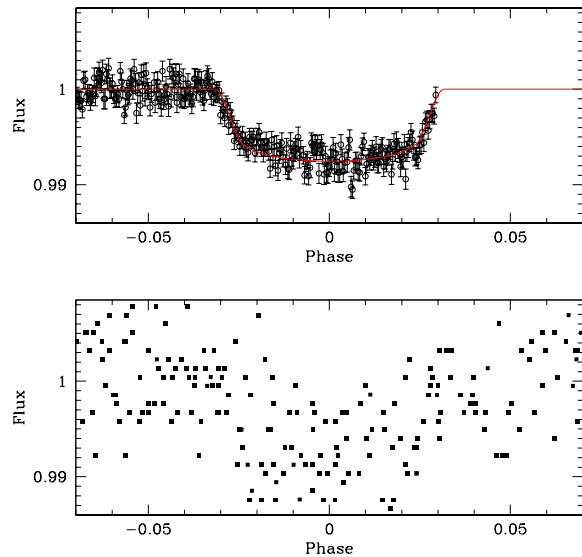


Fig. 2. Top: The best-fit transit curve is shown together with the phased FORS2 data (outliers were removed by 3σ clipping). The error bars show the photon noise. **Bottom:** On the same scale, the OGLE data from 11 individual transits (data from Udalski et al. 2003).

dispersion of the light curve of OGLE-TR-132 before the transit is 1.19 mmag, and the mean photon noise is 1.04 mmag. The dispersion of the residuals during the transit after the transit fit (see below) is 1.14 mmag. We can therefore estimate by quadratically subtracting the photon noise that the systematic effects are smaller than 0.7 mmag. We also checked that colour effects are negligible. Incidentally, this excellent accuracy shows what can be achieved under good conditions at the VLT on a $I = 15.72$ magnitude star.

3.2. Transit fitting

A transit light curve was fitted by least-squares to the photometric data with five free parameters: the radius ratio

Period [days]	1.689857 ± 0.000006
Transit epoch [JD]	$2453142.58884 \pm 0.00009$
Radius ratio	0.0812 ± 0.0017
Impact parameter	0.57 ± 0.10
Transit duration [day]	$0.09476^{+0.00027}_{-0.00007}$
Temperature of primary [K] ^a	6411 ± 179
V-R	0.58 ± 0.05
M_I [mag]	3.05 ± 0.21
age [Gyr]	0 - 1.4
Distance [pc]	2500 ± 250
Primary mass [M_\odot]	1.35 ± 0.06
Primary radius [R_\odot]	1.43 ± 0.10
Planet mass [M_J]	1.19 ± 0.13
Planet radius [R_J]	1.13 ± 0.08
Planet density [$g.cm^{-3}$]	1.02 ± 0.33

Table 1. Parameters for the observed transit, the star OGLE-TR-132 and its planetary companion. ^a: from BPS.

r/R , the transit duration d , the impact parameters b , the period P and the epoch T_0 . A quadratic limb darkening¹ with $u_1 = u_2 = 0.3$ was used (applicable for a late F dwarf according to Barban et al. 2003). The expected transit shape was computed according to Mandel & Agol (2002). The fit was performed in two stages: the transit period was first constrained with the combined OGLE and FORS2 data, which spans over two years. The period was then fixed and the other parameters were fitted on the FORS2 data only. A 3- σ clipping was applied to the data to remove outliers (8 points out of 281) and the uncertainties were scaled from the photon noise with a factor 1.19 for the final fit so that the reduced χ^2 be equal to the number of degrees of freedom. The uncertainties on the parameters were computed from the reduced χ^2 of the combined fit.

The results are given in Table 1 and the fit is shown on Figure 2. The data place very tight constraints on the transit shape. The duration of the transit (defined as the crossing time of the center of the planet through the star's disc) is defined within a few seconds. The shapes of the ingress and egress are also clearly defined, showing the transit to occur at medium latitude on the star. Note that due to the geometry of the problem, the uncertainty distributions are not always symmetrical. For instance, the one-sigma interval for the impact parameter b is 0.44-0.64, but the two-sigma interval is 0.0 - 0.71, so that a central transit is excluded at the two-sigma level by the data².

¹ The data is actually good enough for a linear limb darkening coefficient to be left as a free parameter. Doing this yields $u = 0.6 \pm 0.1$.

² The uncertainty distribution on the physical parameters (mass and radius) is, however, reasonably symmetrical (e.g. a central transit would yield $r = 0.91R_J$)

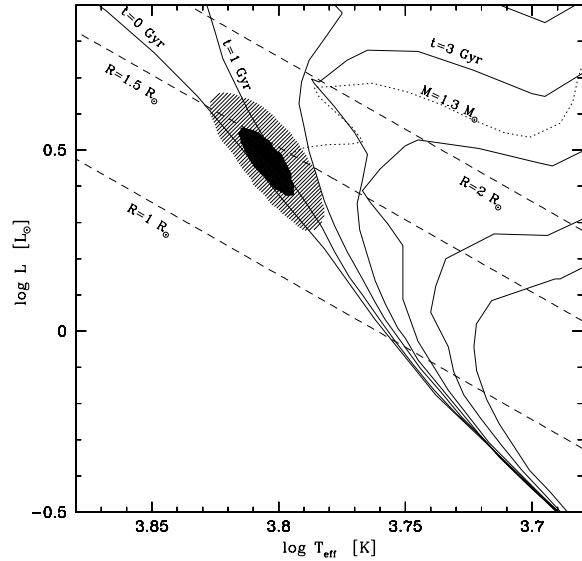


Fig. 3. Position of OGLE-TR-132 in the temperature-luminosity diagram. The 68% (cross-hatched) and 90% (hatched) contours are indicated for the least-squares described in the text. Some landmarks from the Girardi et al. (2002) stellar evolution models are indicated: isochrones of the $z = 0.05$ ($[Fe/H] \sim +0.4$) models for ages 0,1,2,3,5,10,15 Gyr; evolution track for $z = 0.03$ and $M = 1.3M_\odot$. Lines of constant radius at 1, 1.5 and 2 R_\odot are also indicated.

3.3. Radius and mass determination

The radius and mass of OGLE-TR-132 and of its planetary companion can be computed by combining the constraints from the transit curve and from the spectroscopy. Given the very short period, a circular Keplerian orbit can safely be assumed. There are two constraints on the stellar radius and mass:

- The transit duration in phase, which is proportional to $RM^{-1/3}$ for a circular Keplerian orbit.
- The spectroscopic determination of temperature, metallicity and gravity by BPS.

These two constraints were combined by generalised least-squares, assuming that the parameters are confined in the $(T_{eff}, \log g, [Fe/H], M, R)$ space in the sub-manifold defined by an interpolation between the Girardi et al. (2002) stellar evolution models³. The results are given in Table 1 and illustrated in Fig. 3.

This procedure, in addition to M and R , also yields estimates of the stellar age, absolute magnitude and intrinsic colours: $\tau = 0 - 1.4$ Gyr, $M_I = 3.05 \pm 0.21$ mag, $(V - R)_0 = 0.28 \pm 0.02$ mag. Using these values and our measurement of $(V - R)$, we derive $a_v = 1.43 \pm 0.22$ and a distance of 2500 ± 250 pc for OGLE-TR-132.

Our improved period and epoch determination compared to Udalski et al. (2003) also leads to an improved determination of the semi-amplitude of the radial velocity

³ The interpolation was done with the IAC-star software of A. Aparicio, priv. comm.

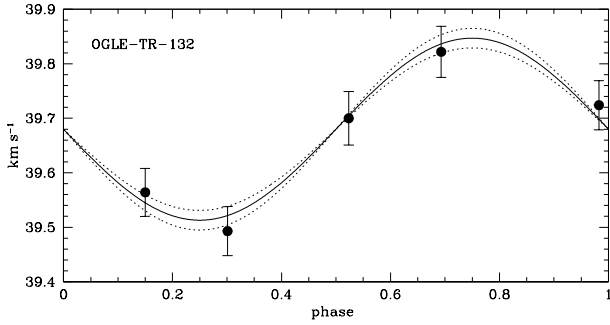


Fig. 4. The radial-velocity measurements of OGLE-TR-132 obtained with VLT/FLAMES (BPS), with the re-evaluated fit. The dotted lines correspond to fit curves for lower and upper $1\text{-}\sigma$ intervals in semi-amplitude K .

orbit, K . We fitted a sinusoidal orbit by least-squares to the radial velocity data with the new period and epoch. The result, $K = 0.167 \pm 0.018$, is plotted in Fig. 4. The new period leads to a significant improvement over the initial value of BPS and to a larger value of K . The phasing of the transit is now in much closer agreement with the variation of the radial velocity. We use this new value in the determination of m from M . The mass m of the planetary companion can be computed from the mass M of the star and K (for a circular orbit, $K \sim m(m+M)^{2/3}$).

The radius r of the planetary companion can be computed from the radius R of the star and the radius ratio r/R . Our values for r and m are given in Table 1.

4. Discussion and conclusion

The planetary transit is thus detected without ambiguity in our FORS2 data set and well sampled in time. From a transit fitting and a new analysis of the VLT/FLAMES radial-velocity curve, we could determine the planet radius and mass with a high accuracy (Table 1). The remaining limitation on the planetary radius precision now results in comparable levels from the systematic residuals in the photometry, the uncertainties in the parent star spectroscopic parameters, and the accuracy of stellar evolution models.

The determination of planet radius and mass give a good estimate of the mean density of OGLE-TR-132b, showing that it is in line with other close-in hot Jupiters, OGLE-TR-56b and OGLE-TR-113b. We confirm the significance of the difference with HD209458b, which has a markedly lower density. Figure 5 shows the mass-radius relationship of the four extrasolar planets where both parameters are measured.

Following Lammer et al. (2003) and Baraffe et al. (2004), we may estimate the mass loss of the OGLE-TR-132 planet due to extreme UV stellar radiation. It would be of the order of $10^{-10} M_J/yr$ if the parent star was of solar type, but it is more likely greater, since the star is hotter and younger (and thus more luminous in the XUV domain) than the Sun. This minimum mass loss estimate is yet twice as large as the mass loss of OGLE-TR-56b

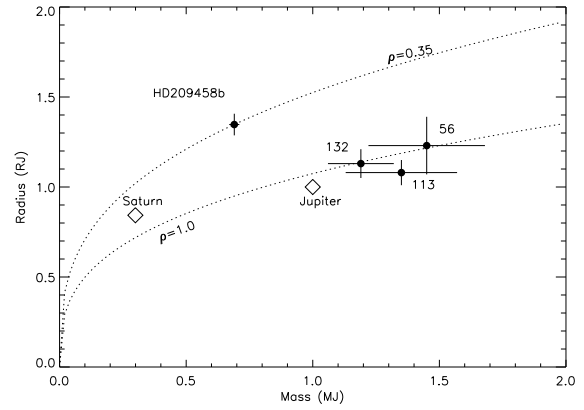


Fig. 5. The mass-radius relationship of the four known transiting planets (from Brown et al., 2001, Cody & Sasselov 2002, BPS, Torres et al. 2004 and this work). OGLE-TR-132 is coded "132", etc... Iso-density lines are also drawn (in units g cm^{-3}). Jupiter and Saturn are shown for comparison.

and four times larger than for HD209458b. We could expect strong signatures of an evaporated exosphere from OGLE-TR-132, larger than those observed in the spectrum of HD209458b (Vidal-Madjar et al., 2003, 2004). Further transit searches and their radial-velocity follow-up will probably provide additional candidates of great interest.

References

- Alard, C. & Lupton, R.H. 1998 ApJ 503, 325
- Alard, C. 2000, A&AS 144, 363
- Baraffe, I., Selsis, F., Chabrier G. et al. 2004, A&A 419, L13
- Barban, C., Goupil, M.J., Van't Veer-Menneret, C. et al. 2003, A&A 405, 1095
- Bouchy, F., Pont, F., Santos, N.C. et al. 2004, A&A 421, L13
- Brown, T.M., Charbonneau, D., Gilliland, R.L. et al. 2001, ApJ 552, 699
- Charbonneau, D., Brown, T. M., Latham, D. W., Mayor, M. 2000, ApJ 529, L45
- Cody, A.M. & Sasselov, D. 2002, ApJ 569, 451
- Girardi, M., Manzato, P., Mezzetti, M., et al. 2002, ApJ 569, 720
- Henry, G. W., Marcy, G., W., Butler, R. P., Vogt, S. S. 2000, ApJ 529, L41
- Konacki, M., Torres, G, Jha, S., Sasselov, D. D. 2003, Nature 421, 507
- Konacki, M., Torres, G., Sasselov, D. D. 2004, ApJ 609, L37
- Kovács, G., Zucker, S., Mazeh, T. 2002, A&A 391, 369
- Lammer, H., Selsis, F., Ribas, I. et al. 2003, ApJ 598, L121
- Mandel, K. & Agol, E. 2002, ApJ 580, 171
- Stetson, P.B., 1987, PASP 99, 191
- Torres, G., Konacki, M., Sasselov, D. & Jha, S., in press
- Udalski, A., Zebrun, K. et al. 2002a, Acta Astron. 52, 115
- Udalski, A., Zebrun, K. et al. 2002b, Acta Astron. 52, 317
- Udalski, A., Pietrzynski, G. et al. 2003, Acta Astron. 53, 133
- Vidal-Madjar A., Lecavelier des Etangs A., Désert J.-M. et al. 2003, Nature 422, 143
- Vidal-Madjar, A., Désert, J.-M., Lecavelier des Etangs, A. et al. 2004, ApJ 604, L69